AEM
Journals.ASM.org

Electron Donors Supporting Growth and Electroactivity of *Geobacter sulfurreducens* Anode Biofilms

Allison M. Speers and Gemma Reguera

Department of Microbiology and Molecular Genetics, Michigan State University, East Lansing, Michigan, USA

Geobacter **bacteria efficiently oxidize acetate into electricity in bioelectrochemical systems, yet the range of fermentation products that support the growth of anode biofilms and electricity production has not been thoroughly investigated. Here, we show that *Geobacter sulfurreducens* oxidized formate and lactate with electrodes and Fe(III) as terminal electron acceptors, though with reduced efficiency compared to acetate. The structure of the formate and lactate biofilms increased in roughness, and the substratum coverage decreased, to alleviate the metabolic constraints derived from the assimilation of carbon from the substrates. Low levels of acetate promoted formate carbon assimilation and biofilm growth and increased the system's performance to levels comparable to those with acetate only. Lactate carbon assimilation also limited biofilm growth and led to the partial oxidization of lactate to acetate. However, lactate was fully oxidized in the presence of fumarate, which redirected carbon fluxes into the tricarboxylic acid (TCA) cycle, and by acetate-grown biofilms. These results expand the known ranges of electron donors for *Geobacter*-driven fuel cells and identify microbial constraints that can be targeted to develop better-performing strains and increase the performance of bioelectrochemical systems.**

The ability of microorganisms to completely oxidize organic compounds to carbon dioxide with an electrode serving as the sole electron acceptor shows promise for the conversion of complex substrates, such as organic wastes and renewable biomass, to electricity and/or biofuels in bioelectrochemical systems (BESs) (19, 20, 26). The degradation of complex substrates in BESs is a multistep process initiated by a fermentative partner, which can be a defined microbial catalyst (34) or a consortium of microorganisms with synergistic activities (19). The activities of the fermentative partner(s) generate complex mixtures of organic acids, such as acetate, lactate, and formate, which accumulate and acidify the fermentation broth, thus inhibiting microbial growth. H_2 is also a major product of the fermentation of organic matter, and its accumulation negatively controls the rate of decomposition (40). Because fermentation end products serve as electron donors for the electrogenic partner, interspecies metabolite transfer contributes greatly to the coulombic efficiencies and electrochemical performance of BESs (6, 14, 30). For this reason, the efficient conversion of fermentation end products to electricity is critical for the efficient processing of complex substrates in BESs.

BESs fed with fermentation products often enrich for exoelectrogens in the *Geobacteraceae* family (16, 26). Key to this enrichment is the ability of *Geobacter* bacteria to grow on the anode electrode as an electroactive biofilm (32). This process requires energy expenditure and sufficient carbon for cell biomass (41) and synthesis of the structural and electronic components of the biofilm matrix, such as electrically conductive pili (31–33) and *c*-type cytochromes associated with an exopolysaccharide (EPS) matrix (36). *Geobacter* bacteria also need to divert some of the electron donor carbon for gluconeogenesis, biomass synthesis, and other anabolic reactions. Thus, electron donor oxidation and assimilation for carbon by *Geobacter* bacteria is ultimately responsible for the electrochemical performance of *Geobacter*-driven BESs. This, in turn, modulates parameters such as biofilm structure and resistance, current density, and mass transfer that limit power production in BESs (39).

Most studies thus far have focused on investigating the electron transfer mechanisms that enable *Geobacter* biofilms to reduce the electrode (25, 32, 35). In contrast, little is known about how electron donors affect the growth and electrochemical performance of *Geobacter* anode biofilms, which is fundamental for design optimization in BESs as well as for the development of better-performing strains. Acetate is the preferred electron donor for *Geobacter* bacteria; it can be oxidized in the tricarboxylic acid (TCA) cycle to produce energy for growth and electrons for electrode reduction while also providing carbon, via its conversion to pyruvate, for gluconeogenesis, biomass synthesis, and other anabolic reactions (41). H_2 also supports current generation in BESs driven by acetate-grown biofilms of the model organism *Geobacter sulfurreducens* (2). However, *G. sulfurreducens* cannot grow autotrophically with CO_2 (9) and needs organic carbon for cell growth (41). For this reason, carbon-containing electron donors are, in principle, necessary to support the growth of anode biofilms in BESs.

The role of formate and lactate as electron donors in BESs is less understood. Both were originally reported not to serve as electron donors for the reduction of Fe(III) (4). However, recent studies demonstrated that lactate could support current generation in a microbial electrolysis cell and could also be oxidized with Fe(III) as an electron acceptor (5). *Geobacter*-like sequences are in fact detected in formate- and lactate-fed BESs (16). Formate and lactate can theoretically produce higher (−0.403 and −0.325 V versus standard hydrogen electrode [SHE], respectively) cell voltages than acetate (−0.277 V versus SHE) (14). However, the performance of formate- and lactate-fed BESs is often reduced com-

Received 2 September 2011 **Accepted** 8 November 2011
Published ahead of print 18 November 2011
Address correspondence to Gemma Reguera, reguera@msu.edu.

doi:10.1128/AEM.06782-11

pared to acetate. For example, power densities in BESs operated under identical conditions but fed different substrates were reportedly higher with acetate (835 ± 20.5 mW/m^2) than with lactate (739 ± 32.2 mW/m^2) and significantly lower with formate (62 ± 0.1 mW/m^2) (15). Furthermore, the power densities matched well with the numerical abundance of *Deltaproteobacteria*, a phylum dominated by *Geobacter* exoelectrogens, in the anode biofilms (acetate, 63%; lactate, 43%; formate, 14%) (15). These results suggested that metabolic constraints associated with the use of formate and lactate by *Geobacter* exoelectrogens limited the performance of the BESs.

Because formate and lactate are often end products of the fermentation of complex substrates and can also theoretically produce higher cell voltages than acetate, we investigated their use as electron donors in BESs driven by the model representative *G. sulfurreducens*. Here, we show that both formate and lactate supported current production in BESs and were oxidized with Fe(III), though with reduced efficiency compared to acetate controls. The reduced performance with formate was due to growth limitations during formate carbon assimilation but could be alleviated by chemical complementation with low levels of acetate. In contrast, lactate carbon assimilation was suboptimal, and cells generated energy for growth through its partial oxidation to acetate. However, providing fumarate as the electron acceptor, which also serves as a carbon source and mobilizes carbon fluxes to the TCA cycle, or sufficient acetate to build the anode biofilms promoted the complete oxidation of lactate and increased BES performance. This expands the known range of electron donors that support the growth and activity of electroactive biofilms of *G. sulfurreducens* in BESs and provides the knowledge necessary to develop strains with improved performance and enrichment protocols that maximize the growth and reductive capabilities of *Geobacter* anode biofilms.

MATERIALS AND METHODS

Bacterial strains and culture conditions. *G. sulfurreducens* PCA was routinely cultured anaerobically in modified fresh water (FW) medium (7) supplemented with 1 μM Na_2SeO_4 to promote growth and with acetate (15 mM) and fumarate (40 mM) as the electron donor and acceptor, respectively. Growth with other electron donors was tested by replacing acetate with 10 mM D,L-lactate, 30 mM formate, or 60 mM formate and measuring the culture's turbidity spectrophotometrically at 600 nm. When indicated, fumarate was replaced with 56 mM Fe(III)-citrate as the electron acceptor, and growth was monitored by measuring the amount of HCl-extractable Fe(II) resulting from the reduction of Fe(III) (21). *Shewanella oneidensis* MR-1, which was used as a control for lactate dehydrogenase activity, was routinely cultured in tryptic soy broth (30 g/liter). All cultures were incubated at 30°C.

BESs. Cultures used as inoculum for bioelectrochemical systems (BESs) were grown in anaerobic mineral medium (38) supplemented with 10 ml/liter vitamin mix (1) (herein referred to as DB medium) with acetate (20 mM) and fumarate (40 mM) serving as the electron donor and acceptor, respectively. The BESs consisted of dual-chambered, H-type fuel cells with the anode and cathode chambers separated by a Nafion membrane (Ion Power, Inc., New Castle, DE) and each containing 90 ml of DB medium and an electron donor (1 mM acetate, 4 mM formate, 0.67 mM D,L-lactate). For BESs with H_2, 8.8 ml of sterile H_2 gas was added to the headspace of the anode chamber to provide 0.36 mmol H_2 or the same the same number of electrons (0.72 mmol) as in 90 ml of 1 mM acetate. When indicated, BESs were also supplemented with 0.1 mM acetate. Alternatively, anode biofilms were grown with 1 mM acetate until depleted, and then the medium of the anode chamber was replaced inside a glove box chamber (Coy Laboratory Products, Inc., Grass Lake, MI) with fresh medium containing 0.67 mM lactate. Graphite rod electrodes (Alfa Aesar, 1.27-cm diameter, 99% metals basis, 12 cm^2) served as the working (anode) and counter (cathode) electrodes. A VSP potentiostat (BioLogic, Claix, France) was used to set a 0.24-V potential at the anode electrode versus a 3 M Ag/AgCl reference electrode (Bioanalytical Systems, Inc., West Lafayette, IN). Both chambers were made anoxic and buffered to pH 7 by continuous sparging with N_2-CO_2 (80:20). A 40% (vol/vol) inoculum of early-stationary-phase cells grown at 30°C in DB medium with acetate and fumarate was harvested by centrifugation (4,000 × *g*, 8 min, 25°C), washed once, and resuspended in 10 ml of DB medium before inoculating into the 90 ml of sterile DB medium contained in the anode chamber. Supernatant samples were periodically removed to monitor electron donor removal and formation of metabolic intermediates, as described in detail in the "Analytical techniques" section.

CLSM and COMSTAT analyses. The anode biofilms were examined microscopically using a FluoView FV1000 inverted microscope system (Olympus, Center Valley, PA) equipped with an UPLFLN 40× oil immersion objective (Olympus; numerical aperture [NA], 1.30). For these analyses, the anode electrodes were removed from the BESs once the current had dropped to zero, and the biofilm cells were differentially stained live (green) and dead (red) with the BacLight viability kit (Invitrogen, Carlsbad, CA) by following the manufacturer's recommendations. The anode electrode was placed on a Lab-Tek coverglass chamber (Nunc, Rochester, NY) filled with 3 ml 1× phosphate-buffered saline (PBS) and imaged by confocal laser scanning microscopy (CLSM) at excitation wavelengths of 488 nm (SYTO 9, live cells) and 543 nm (propidium iodide, dead cells). Emission from SYTO 9 was detected with a BA505-525 bandpass filter and from propidium iodide with a BA560IF longpass filter. Image stacks were collected every 1 μm, and three-dimensional image projections were produced using the FV10-ASW 3.0 software (Olympus). Image stacks were taken from approximately 8 random fields (1,024 by 1,024 pixels, 0.31 μm/pixel) per electrode, and a minimum of two BES replicates were examined for each electron donor tested. The structure of the anode biofilm was analyzed using COMSTAT image analysis software, as previously described (13). Connected volume filtration was used to remove noise in the data from cells not attached to the substratum.

Lactate dehydrogenase and protein assays. *G. sulfurreducens* cells were grown in 100 ml of DB medium supplemented with 10 mM D,L-lactate. *S. oneidensis* MR-1 was also grown in 100 ml of DB medium but prepared aerobically, buffered with 1,4-piperazinediethanesulfonic acid (PIPES) rather than bicarbonate, and supplemented with 45 mM D,L-lactate. Mid-exponential-phase cells (optical density at 600 nm [OD_{600}] of 0.3 to 0.5) were harvested by centrifugation (4,000 × *g*, 20 min, 4°C), washed twice, and resuspended in 20 mM HEPES buffer (pH 7, 100 mM NaCl, 2 mM β-mercaptoethanol), as described before (29). The cells were then lysed by sonication using a Branson Sonifier 450 (5 times, 1 min, 50% duty cycle, in an ice-water bath). The rate of D- and L-lactate-oxidizing activity coupled to the reduction of phenazine methosulfate (PMS) and 3-(4,5-dimethylthiazolyl-2-)2,5-diphenyltetrazolium bromide (MTT) was measured spectrophotometrically at 570 nm, as previously described (29). A unit (U) of lactate dehydrogenase activity was defined as the amount of enzyme that reduces 1 nmol of MTT per min. The enzyme activity was normalized to the total cell protein, which was measured by solubilizing the sonicated cell extracts with 1/2 vol of 2 N NaOH at 100°C for 1 h, neutralizing with 1/2 vol of 2 N HCl, and measuring the protein concentration with the reducing agent compatible Pierce bicinchoninic acid (BCA) protein assay kit (Thermo Scientific, Rockford, IL) and bovine serum albumin (BSA) as the standard.

Analytical techniques. Culture supernatant fluids were filtered (0.45-μm-syringe filters; National Scientific, Rockwood, TN) and analyzed by high-performance liquid chromatography (HPLC) (Waters, Milford, MA) at 30°C, as previously described (23).

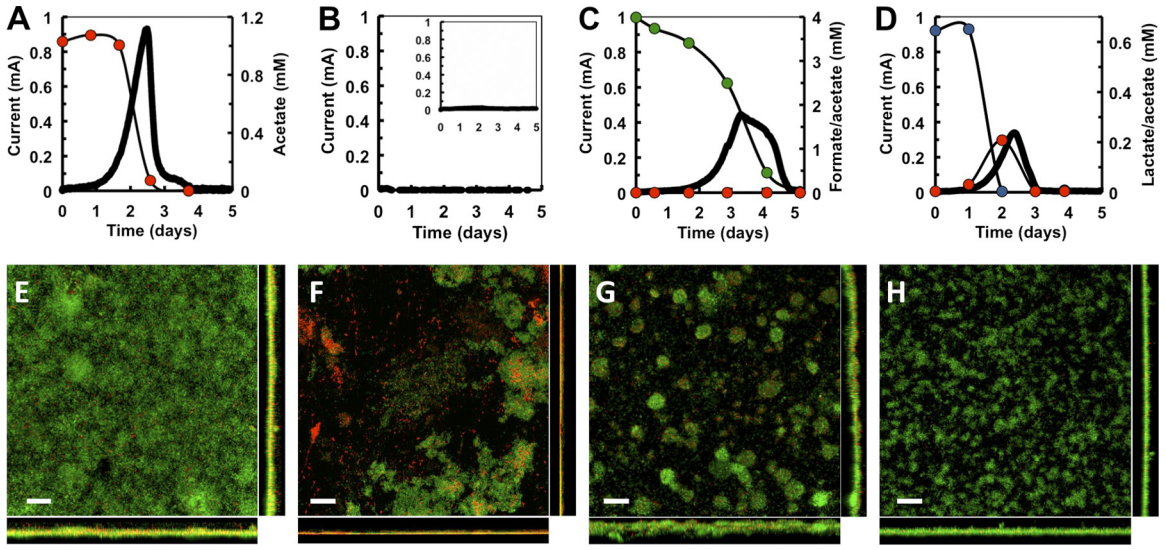

FIG 1 Current generation (solid line) and electron donor uptake (circles [red, acetate; green, formate; blue, lactate]) (A to D) and CLSM micrographs of anode biofilms (E to H) in fuel cells fed with acetate (A and E), H_2 (B and F), formate (C and G), or lactate (D and H). The inset in panel B shows controls with no electron donor. The biofilms in panels E to H were stained with the BacLight viability dyes (green, live cells; red, dead cells). Top views and the corresponding projections in the *x* (bottom) and *y* (right) axes are shown. Scale bar, 20 μm.

RESULTS AND DISCUSSION

Current generation from formate and lactate. We investigated the electrical conversion of formate and lactate by *G. sulfurreducens* in BESs in reference to acetate. The electron donors were provided as equimolar supplies of electrons (1 mM acetate, 4 mM formate, and 0.67 mM lactate). The anode was poised at a constant potential of 240 mV versus Ag/AgCl to maintain consistency between different fuel cells, remove any potential limitations from electron transfer at the cathode, and eliminate the possibility of oxygen intrusions into the anode chamber (2) that might support aerobic growth (18). Current production with acetate increased linearly after a short lag phase (Fig. 1A), as the planktonic cells from the inoculum attached to the electrode and grew with constant doubling times while oxidizing acetate and producing electricity (22). The rate of current increase, which correlates with the exponential phase of biofilm growth (22), averaged 0.12 mA h^{-1} in triplicate BESs and reached a maximum current current of ca. 0.81 mA (Table 1) before declining as the acetate was depleted (Fig. 1A). Coulombic efficiencies were ca. 80% (Table 1), indicating that on average 80% of the acetate was converted into current, while the remaining substrate was used for cell biomass. In contrast, negative controls with H_2 or without electron donor failed to support biofilm growth and current generation (Fig. 1B).

The rates of current increase in formate-fed BESs were similar to the acetate-fed systems (Fig. 1C and Table 1), suggesting that the growth rates of the biofilm cells were similar to acetate biofilms. However, the maximum current was almost half of that obtained with acetate (Table 1), and current production declined slowly while the formate was consumed (Fig. 1C). Coulombic efficiencies (93%) were higher in formate-fed than in acetate-fed systems (Table 1), suggesting that over time the anode biofilms converted more formate to electricity than acetate yet at a lower rate. These results suggested that formate carbon assimilation, rather than oxidation, limited BES performance.

Lactate also supported similar rates of current increase (Fig. 1D and Table 1). Although all the lactate was removed from the culture broth (Fig. 1D), the maximum current and coulombic efficiencies were lower with lactate than with acetate and formate (Table 1). Interestingly, lactate uptake was coupled to the accumulation of acetate in the culture broth, which was used to support current production once all the lactate had been exhausted (Fig. 1D). This suggests that lactate was partially oxidized to acetate. This is similar to what has been reported for *S. oneidensis* grown anaerobically in microbial fuel cells (17). As lactate has three carbons and acetate has two, the maximum theoretical lactate-acetate ratio is 1:1.5. However, we measured 0.4 mol of acetate for every mol of lactate consumed. This suggests that most of the lactate was diverted to cell biomass, rather than electricity production, during growth on the anode. This is consistent with the coulombic efficiencies calculated for the lactate-fed BESs, which indicated that on average only 38% of the lactate was converted into electricity (Table 1).

Biofilm biomass and structure in formate- and lactate-fed BESs. Current generation by *G. sulfurreducens* is directly proportional to the growth of the anode biofilms on the electrode (32).

TABLE 1 Performance of BESs of *G. sulfurreducens* fed with different electron donors

Electron donor	Rate of current increase (mA h^{-1})	Maximum current (mA)	CE[a] (%)
Acetate	0.12 ± 0.01	0.81 ± 0.05	80 ± 3
Formate	0.12 ± 0.01	0.48 ± 0.04	93 ± 1
Lactate	0.12 ± 0.01	0.33 ± 0.01	38 ± 1
Formate[b]	0.12 ± 0.01	0.90 ± 0.03	75 ± 1
Lactate[b]	0.13 ± 0.01	0.37 ± 0.02	44 ± 1
Lactate[c]	0.09 ± 0.01	0.81 ± 0.01	90 ± 1

[a] CE, coulombic efficiency.
[b] Supplemented with 0.1 mM acetate.
[c] Biofilms grown with 1 mM acetate before the addition of medium containing 0.67 mM lactate.

TABLE 2 Anode biofilm structure as a function of the electron donor

Electron donor	Total biomass ($\mu m^3/\mu m^2$)	Average thickness (μm)	Roughness coefficient (0 to ∞)	Surface-to-vol ratio ($\mu m^2/\mu m^3$)	Substratum coverage (%)
Acetate	25.8 ± 3.2	26.7 ± 3.9	0.1 ± 0.1	0.8 ± 0.3	99.9 ± 0.1
Formate	13.7 ± 1.9	21.7 ± 4.1	0.3 ± 0.1	1.9 ± 0.4	75.0 ± 12.2
Lactate	13.0 ± 3.8	16.0 ± 3.6	0.2 ± 0.1	1.6 ± 0.7	91.0 ± 7.6
H_2	2.9 ± 0.6	10.2 ± 3.3	1.0 ± 0.2	2.0 ± 0.4	37.2 ± 9.2
Formate[a]	25.5 ± 8.4	26.9 ± 9.4	0.2 ± 0.1	0.9 ± 0.3	99.3 ± 0.6
Lactate[a]	17.9 ± 3.6	18.9 ± 2.7	0.1 ± 0.1	1.2 ± 0.7	97.2 ± 3.9

[a] Supplemented with 0.1 mM acetate.

This requires energy from the oxidation of electron donors as well as from assimilation of some of the electron donor carbon through gluconeogenesis, biomass synthesis, and other anabolic activities (41). Because the structural organization of the biofilm is highly responsive to carbon use efficiency (13), we used the COMSTAT statistic software (13) to quantitatively analyze the structure of the anode biofilms as a function of the electron donor. Figures 1E to H show representative fields obtained by CLSM. Changes in biofilm structure were readily apparent in the CLSM micrographs. The acetate biofilms had confluent growth and very few dead cells (Fig. 1E), whereas the H_2 biofilms had many dead cells and cell aggregates with no defined structure (Fig. 1F). In contrast, the formate and lactate biofilms were porous and patchy and composed of small microcolonies, which were smaller and denser in the lactate biofilms (Fig. 1G and H). Table 2 shows the structural parameters analyzed in the biofilms: total biomass (calculated as biovolume per surface area), mean biofilm thickness, roughness coefficient (variations in the biofilm thickness and, therefore, an indicator of biofilm heterogeneity), surface-to-biovolume ratio (portion of the biofilm that is exposed to nutrient flow), and substratum coverage (the area of the electrode occupied by the biofilm biomass). Because acetate-fed biofilms had the best performance (Fig. 1A), their structural parameters were used as a reference. The anode biofilms formed in the H_2 BESs (Fig. 1B) were used as negative controls. The most notable variations were decreases in total biofilm biomass and thickness from fuel cells fed with the different substrates, which correlated well with the observed decreases in maximum current ($R^2 = 0.973$ and $R^2 = 0.977$, respectively). Coulombic efficiencies for formate were higher than for any other electron donor, including acetate (Table 1). Thus, less formate was used for cell biomass, and the biofilm biomass and thickness were reduced compared to acetate biofilms (Table 2). Lactate biofilms also had reduced biomass and thickness (Table 2) and low coulombic efficiencies (Table 1). This suggests that both lactate oxidation and assimilation for carbon limited biofilm growth and current generation.

The roughness and the surface-to-volume ratio increased, and the substratum coverage decreased, in the formate and lactate biofilms (Table 2). The biofilm heterogeneity (measured as roughness) was inversely proportional to the substratum coverage ($R^2 = 0.966$). This shows that the structural organization of the anode biofilms was highly responsive to the electron donor. The preferred electron donor, acetate, supported the highest yields of biofilm growth and allowed for the formation of thicker, relatively uniform, confluent biofilms. This maximized electrode coverage and cell stacking per electrode surface area. In contrast, metabolic constraints associated with the use of formate or lactate prevented optimal biofilm growth. As a result, the biofilms were more porous and heterogeneous, which increased nutrient flow and minimized diffusion limitations but reduced the electrode coverage. This is in agreement with mathematical models of biofilm growth that support the notion that the biofilm structure adapts to the availability of nutrients. For example, biofilm growth is predicted to be slower at lower concentrations of nutrients due to diffusion limitations. Models show that low concentrations of nutrients, and therefore slow growth, result in porous biofilms composed of channels and interstitial voids, whereas saturating concentrations of nutrients and rapid growth result in the formation of thick, compact, and uniform biofilms (27, 28). Hence, the increases in roughness and surface-to-volume ratios measured with formate and lactate reflected the lower biofilm growth yields compared to acetate.

Formate and lactate as electron donors with Fe(III) and fumarate. As the standard redox potential ($E°$) of the half reaction of $Fe^{3+} + e^- \rightarrow Fe^{2+}$ ($E^0 = 771$ mV versus SHE) is higher than the potential (450 mV versus SHE or 240 mV versus 3 M Ag/AgCl) used in the BES experiments (Fig. 1), a higher electromotive force (ΔE^0) and, therefore, more energy for growth and more electrons available for reductive reactions are theoretically possible for the electron donor/Fe(III) coupling than for the electron donor/electrode pair. Thus, we investigated if formate and lactate could support cell growth in cultures with Fe(III) citrate as the sole electron acceptor. For these experiments, cells were harvested by centrifugation and washed prior to inoculation to prevent any nutrient carryover. As shown in Fig. 2A, cultures supplemented with 30 mM formate (concentrations like those previously tested [4]) grew and reduced all the Fe(III), though doubling times (17.3 ± 7.9 h) were higher than those supplemented with equimolar concentrations of carbon in the 15 mM acetate controls (9.7 ± 0.2 h). Increasing the concentration of formate to 60 mM to provide the same amount of electrons as in 15 mM acetate did not improve growth but rather slowed it down, with generation times in triplicate cultures averaging 45.1 (±6.1) h. These results demonstrate that, in contrast to early reports (4), the coupling of formate oxidation to Fe(III) is possible, yet growth with formate is slower than with acetate. In contrast, formate (30 mM) did not support growth with the intracellular electron acceptor fumarate (Fig. 2B). Higher concentrations of formate (60 mM) also failed to support growth (data not shown). Furthermore, less than 10% of the formate was removed from the supernatants of the 30 mM and 60 mM formate cultures. The standard redox potential of the fumarate^{2-} + 2 e^- + 2H^+ → succinate^{2-} ($E° = 31$ mV versus SHE) is significantly lower than the Fe(III)/Fe(II) pair and the electrode potential that supported the formate-to-current BES reaction (Fig. 1). As a result, the formate/fumarate coupling did not gen-

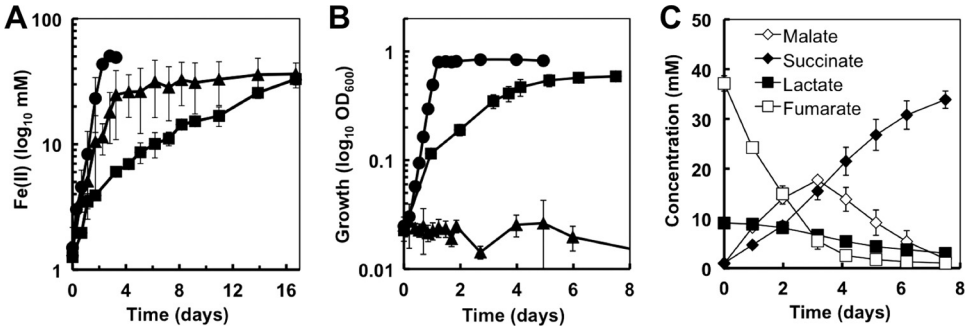

FIG 2 Iron reduction (A) and growth (B) of *G. sulfurreducens* with acetate (circles), formate (triangles), or lactate (squares) as the electron donor and Fe(III) citrate (A) or fumarate (B) as the electron acceptor. (C) Lactate oxidation coupled to fumarate reduction and generation of malate and succinate in lactate-fumarate cultures shown in panel B.

erate as much energy for cell growth as the formate/Fe(III) coupling.

As with the formate studies, we investigated if the more energetically favorable lactate/Fe(III) coupling was possible. After an extended lag phase (ca. 2 days), cells started to grow exponentially and reduced the available Fe(III) citrate (Fig. 2A). However, average doubling times with lactate (90 ± 12 h) were ca. 5- and 9-times greater than with formate and acetate, respectively. Hence, although at high-enough redox potential *G. sulfurreducens* can also use lactate as an electron donor, growth is slower than with acetate or formate. Interestingly, lactate also supported growth in cultures with fumarate (Fig. 2B). Fumarate has a lower redox potential than Fe(III) and, theoretically, less energy for growth, and fewer electrons for reductive reactions are expected for the lactate/fumarate coupling. Yet, growth was stimulated (doubling time, 35 ± 2 h) in the fumarate cultures (Fig. 2B) compared to in the Fe(III) cultures (Fig. 2A). Furthermore, lactate oxidation was coupled to the reduction of fumarate to succinate, but acetate was not detected (Fig. 2C). These results suggested that lactate was completely oxidized to CO_2. Approximately 90% of the electrons in the lactate consumed (73 ± 2) were recovered as succinate (66 ± 2), and malate was also detected (Fig. 2C). Approximately 7% (±3%) of the fumarate was not recovered as succinate (Fig. 2C). This is in agreement with metabolic flux analyses of acetate-fumarate cultures that indicate that less than 10% of the fumarate is used as a source of carbon (41). Fumarate enters the TCA cycle to generate malate, which can then be converted into oxaloacetate and phosphoenolpyruvate for gluconeogenesis. Malate and oxaloacetate intermediates can also generate pyruvate to replenish acetyl coenzyme A (acetyl-CoA) for oxidation in the TCA cycle (41). In fact, some low levels of pyruvate (<1 mM) also accumulated in the culture over time. Oxaloacetate can also be condensed with acetyl-CoA to produce citric acid, a reaction catalyzed by the citrate synthase enzyme of the TCA cycle (3). This provides a route for lactate-derived acetyl-CoA to be fully oxidized in the TCA cycle when fumarate is the electron acceptor.

Metabolic constraints associated with the assimilation of formate carbon. Acetate and formate are oxidized and assimilated for carbon using different metabolic pathways. As shown in Fig. 3, most of the energy derived from acetate comes from its oxidation through the TCA cycle, while its assimilation as carbon is derived from gluconeogenesis via pyruvate (41). In contrast, formate oxidation in *G. sulfurreducens* is predicted to be catalyzed by a periplasmically oriented, membrane-bound formate dehydrogenase (FDH) enzyme complex (24), which shows similarity to the nitrate-inducible formate dehydrogenase (Fdh-N) that couples formate oxidation and nitrate reduction in *Escherichia coli* (8). Genome analyses also predict that formate carbon can be assimilated in the reaction of the pyruvate formate lyase (PFL) (24), which uses formate and acetyl-CoA as substrates to produce pyruvate and CoA (Fig. 3). Previous studies (37) suggested that the PFL reaction may not be functional in the direction toward formate synthesis. Yet, whether this reaction can function in the opposite direction for formate carbon assimilation has never been investigated. As acetate can provide acetyl-CoA for the PFL reaction, we investigated the efficiency of formate carbon assimilation as pyruvate by supplementing formate-fed BESs with low concentrations (0.1 mM) of acetate, which were previously shown to provide a sufficient amount of carbon for cell growth with H_2 as an electron donor (9). The small amount of acetate rescued the growth defect with formate (Fig. 4A) and supported similar rates of current increase and maximum current as in acetate-fed BESs (Table 1). Furthermore, formate and acetate were removed from the culture broth concomitantly (Fig. 4B), consistent with formate carbon being coassimilated with acetyl-CoA in the PFL reaction. Coulombic efficiencies in formate-fed BESs supplemented with acetate (75%) were also lower than those measured with formate only (Table 1). Thus, less formate was being used as an electron donor for electricity generation, and more was being diverted for cell biomass. The addition of acetate also promoted the confluent

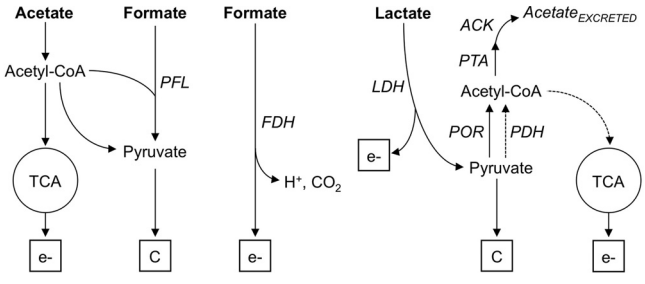

FIG 3 Metabolic routes for the oxidation ($e\bar{v}$) and carbon assimilation (C) of acetate, formate, and lactate (in bold). Alternative routes predicted to also be operative when fumarate serves as the electron acceptor are shown with dashed lines. Enzyme abbreviations: *PFL*, pyruvate formate lyase; *FDH*, formate dehydrogenase; *ACK*, acetate kinase; *PTA*, phosphotransacetylase; *PDH*, pyruvate dehydrogenase; *POR*, pyruvate oxidoreductase; *LDH*, lactate dehydrogenase.

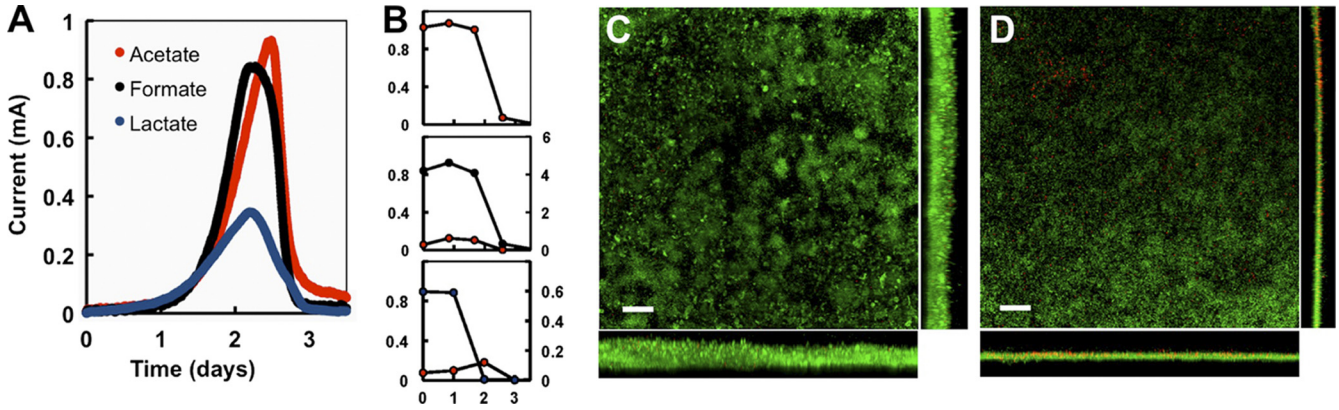

FIG 4 (A and B) Effect of acetate supplementation (0.1 mM) on current generation (A) and substrate uptake (B) in fuel cells with acetate (red), formate (black), and lactate (blue). Left axes in panel B, acetate in mM; right axes, formate or lactate in mM; *x* axes, time in days. (C and D) CLSM micrographs of the anode biofilms from formate (C) and lactate (D) fuel cells supplemented with 0.1 mM acetate. The biofilms were stained with the BacLight viability dyes (green, live cells; red, dead cells). Top views and the corresponding projections in the *x* (bottom) and *y* (right) axes are shown. Scale bar, 20 μm.

growth of the anode biofilms, whose height and biomass increased to levels comparable to the acetate controls (Fig. 4C and Table 2). The biofilms were more uniform and did not increase the surface area exposed to nutrient flow, as indicated by the lower roughness coefficient and surface-to-biovolume ratio (Table 2). Substrate coverage also increased and was saturating. As the thickness of the biofilm is directly proportional to the maximum current (32), alleviating the metabolic constraints associated with the assimilation of formate carbon promoted the growth of confluent biofilms (Fig. 4C) and maximized electrode coverage (Table 2) and BES performance (Fig. 4A).

Lactate oxidation and assimilation for carbon in *G. sulfurreducens*. Lactate is oxidized and assimilated independently of acetate (Fig. 3). Consistent with this, supplementing the BESs with small amounts of acetate (0.1 mM) had no significant effects on performance (Fig. 4A) or in lactate-acetate stoichiometry (Fig. 4B) but improved coulombic efficiencies (Table 1), as current was also generated from the acetate oxidation. Biofilm structural parameters, such as roughness and surface-to-biovolume ratio, were also similar to the acetate-fed biofilms (Table 2). Substrate coverage also increased and was mostly saturating (Table 2). However, the biofilm biomass and thickness, though greater than in lactate-only BESs, were lower than those in acetate biofilms (Table 2). In contrast, lactate was fully oxidized by acetate-grown anode biofilms (Fig. 5A). Furthermore, the maximum current and coulombic efficiencies increased to levels comparable to acetate biofilms (Table 1). The biofilms maintained the confluent growth and maximum substrate coverage of acetate biofilms (Fig. 5B). Thus, lactate can be fully oxidized by the anode biofilms once the carbon demands are satisfied.

Lactate oxidation and assimilation for carbon are initiated in the reaction catalyzed by the lactate dehydrogenase (LDH) enzyme (Fig. 3). Although the genome of *G. sulfurreducens* does not contain an annotated LDH gene (24), comparative genomic analyses identified an operon (*ldhEFG*) encoding proteins homologous to the multisubunit lactate oxidase of *S. oneidensis* MR-1 (29). We identified a homologous region in the *G. sulfurreducens* genome in genome-wide comparisons of the *ldhEFG* region of *S. oneidensis* by using the tools available at the Comprehensive Microbial Resource website (http://cmr.jcvi.org/tigr-scripts/CMR/CmrHomePage.cgi). The region includes genes (*GSU1622* to *GSU1624*) encoding an L-lactose permease, a GlcD flavoprotein, and the Fe-S subunit of a putative glycolate oxidase (GO) enzyme and is conserved in other *Geobacter* genomes, such as *Geobacter uraniireducens* and *Geobacter metallireducens*. GO is a peroxisomal enzyme of plants and cyanobacteria that shares remarkable

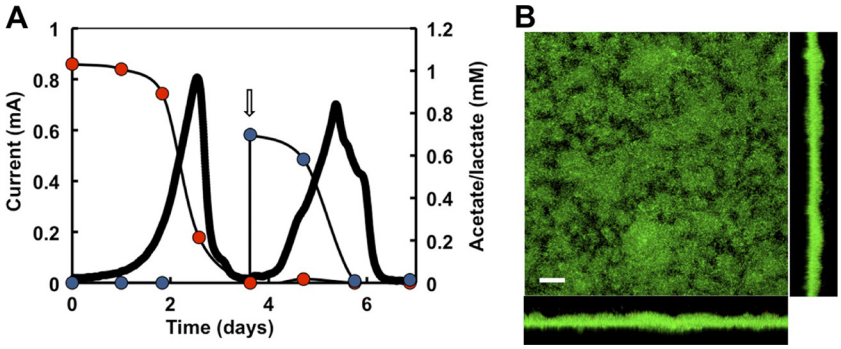

FIG 5 Lactate oxidation by acetate-grown biofilms in BESs. (A) Current generation coupled to acetate and then lactate use as electron donors. The addition of lactate to the anode chamber is shown with an arrow. (B) CLSM micrograph of lactate-oxidizing anode biofilms previously grown with acetate. The biofilms were stained with the BacLight viability dyes (green, live cells; red, dead cells). Top view and the corresponding projections in the *x* (bottom) and *y* (right) axes are shown. Scale bar, 20 μm.

structural homology with LDH and other flavoproteins that catalyze dehydrogenation reactions (11). As a result, GO can catalyze the oxidation of lactate yet at a lower rate (12). Consistent with this, D-LDH and L-LDH activities (99 ± 16 and 128 ± 10 U/mg protein, respectively) in cell extracts of *G. sulfurreducens* grown with lactate and fumarate were significantly lower than in cell extracts of *S. oneidensis* MR-1 (848 ± 95 and 331 ± 42 U/mg protein, respectively).

The activity of the LDH enzyme converts lactate into pyruvate, which can then be converted into acetyl-CoA by the pyruvate ferredoxin oxidorreductase (POR) enzyme (Fig. 3). However, the POR reaction is slow in the pyruvate–to–acetyl-CoA direction (37) and lactate-derived pyruvate is predicted to accumulate inside the cell, thereby creating an excess flux of carbon and limiting growth. *E. coli* balances excess fluxes of carbon and generates energy for growth by diverting the excess carbon as acetyl-CoA substrate for the acetate kinase (ACK)/phosphotransacetylase (PTA) pathway, which results in the excretion of acetate and the generation of ATP (10). The ACK/PTA pathway is also present in *G. sulfurreducens* (37) and provides a two-step reaction to partially oxidize lactate to acetate and gain energy for growth (Fig. 3). In contrast to the partial oxidation of lactate in BESs (Fig. 1D), lactate was fully oxidized in cultures with fumarate (Fig. 2C). This is because fumarate carbons are used through alternative pathways (Fig. 3), such as the reaction catalyzed by the pyruvate dehydrogenase (PDH), which replenishes acetyl-CoA, and the generation of oxaloacetate from fumarate-derived malate (41). Acetyl-CoA and oxaloacetate are then condensed in the reaction catalyzed by the citrate synthase enzyme of the TCA cycle. This allows lactate to be completely oxidized when fumarate is the electron acceptor.

Implications. The results presented herein demonstrate that *G. sulfurreducens* has a broader range of electron donors than originally reported (4). They also provide insights into the limitations reported for *Geobacter*-driven BESs fed with fermentation end products such as acetate, lactate, and formate (16). Although higher voltages are predicted for formate and lactate than acetate (14), acetate-fed fuel cells produce higher power densities than lactate-fed fuel cells and significantly higher power densities than formate-fed fuel cells operated under identical conditions (15). This is because acetate supports optimal biofilm growth and current production in *Geobacter* bacteria. Lactate oxidation to pyruvate, which is a poor electron donor for *G. sulfurreducens* (37), creates an excess flux of carbon inside the cells and limits growth. As a result, lactate is partially oxidized to acetate in BESs. Thus, slower growth is predicted for *G. sulfurreducens*-like organisms during enrichments with lactate. However, the performance of BESs can be improved by adding carbon sources that alleviate the excess carbon fluxes and promote the complete oxidation of lactate in the TCA cycle. Formate oxidation was also coupled to current production, yet BES performance was limited by formate carbon assimilation in the PFL reaction. This provides a plausible explanation for the finding that anode biofilms from formate-fed BESs are dominated by low-power-producing *Paracoccus* species and harbor only a small percentage (14%) of high-power-producing *Geobacter*-like members (15). *Paracoccus* spp. can efficiently oxidize formate to CO_2 and H_2 (15). Although both H_2 and formate can be used as electron donors by exoelectrogens like *G. sulfurreducens*, a carbon source is required to build the biofilm cell biomass. Hence, *Geobacter* spp. are outcompeted on the anode electrode by low-power-producing organisms (15). However, the growth of *Geobacter* spp. with formate could be stimulated by providing small amounts of acetate in the inoculum to promote the assimilation of formate carbon to support biofilm growth on the anode electrode. Taken together, these results highlight the importance of selecting combinations of electron donors that promote the growth and establishment of *Geobacter* anode biofilms. This information can be applied to develop better-performing strains and to manipulate the microbial and metabolic diversity of anode biofilms for increased power production from defined substrates in BESs.

ACKNOWLEDGMENTS

This work was supported by a Strategic Partnership grant from the MSU Foundation to G.R. and a Marvin Hensley Endowed fellowship and a continuation fellowship from the College of Natural Science at Michigan State University to A.M.S. Support from the Michigan Economic Development Corporation is also acknowledged.

We thank Melinda Frame and Bryan Schindler for support during different phases of this work.

REFERENCES

1. **Balch WE, Fox GE, Magrum LJ, Woese CR, Wolfe RS.** 1979. Methanogens: reevaluation of a unique biological group. Microbiol. Rev. **43**:260–296.
2. **Bond DR, Lovley DR.** 2003. Electricity production by *Geobacter sulfurreducens* attached to electrodes. Appl. Environ. Microbiol. **69**:1548–1555.
3. **Bond DR, et al.** 2005. Characterization of citrate synthase from *Geobacter sulfurreducens* and evidence for a family of citrate synthases similar to those of eukaryotes throughout the *Geobacteraceae.* Appl. Environ. Microbiol. **71**:3858–3865.
4. **Caccavo F, Jr, et al.** 1994. *Geobacter sulfurreducens* sp. nov., a hydrogen- and acetate-oxidizing dissimilatory metal-reducing microorganism. Appl. Environ. Microbiol. **60**:3752–3759.
5. **Call DF, Logan BE.** 14 October 2011. Lactate oxidation coupled to iron or electrode reduction by *Geobacter sulfurreducens* PCA. Appl. Environ. Microbiol. [Epub ahead of print.] doi:10.1128/AEM.06434-11.
6. **Call DF, Wagner RC, Logan BE.** 2009. Hydrogen production by *Geobacter* species and a mixed consortium in a microbial electrolysis cell. Appl. Environ. Microbiol. **75**:7579–7587.
7. **Cologgi DL, Lampa-Pastirk S, Speers AM, Kelly SD, Reguera G.** 2011. Extracellular reduction of uranium via *Geobacter* conductive pili as a protective cellular mechanism. Proc. Natl. Acad. Sci. U. S. A. **108**: 15248–15252.
8. **Coppi MV.** 2005. The hydrogenases of *Geobacter sulfurreducens*: a comparative genomic perspective. Microbiology **151**:1239–1254.
9. **Coppi MV, O'Neil RA, Lovley DR.** 2004. Identification of an uptake hydrogenase required for hydrogen-dependent reduction of Fe(III) and other electron acceptors by *Geobacter sulfurreducens.* J. Bacteriol. **186**: 3022–3028.
10. **el-Mansi EM, Holms WH.** 1989. Control of carbon flux to acetate excretion during growth of *Escherichia coli* in batch and continuous cultures. J. Gen. Microbiol. **135**:2875–2883.
11. **Fraaije MW, Mattevi A.** 2000. Flavoenzymes: diverse catalysts with recurrent features. Trends Biochem. Sci. **25**:126–132.
12. **Frederick SE, Gruber PJ, Tolbert NE.** 1973. The occurrence of glycolate dehydrogenase and glycolate oxidase in green plants: an evolutionary survey. Plant Physiol. **52**:318–323.
13. **Heydorn A, et al.** 2000. Quantification of biofilm structures by the novel computer program COMSTAT. Microbiology **146**(Part 10):2395–2407.
14. **Kiely PD, Call DF, Yates MD, Regan JM, Logan BE.** 2010. Anodic biofilms in microbial fuel cells harbor low numbers of higher-power-producing bacteria than abundant genera. Appl. Microbiol. Biotechnol. **88**:371–380.
15. **Kiely PD, Rader G, Regan JM, Logan BE.** 2011. Long-term cathode performance and the microbial communities that develop in microbial fuel cells fed different fermentation end products. Bioresour. Technol. **102**:361–366.
16. **Kiely PD, Regan JM, Logan BE.** 2011. The electric picnic: synergistic requirements for exoelectrogenic microbial communities. Curr. Opin. Biotechnol. **22**:378–385.

17. **Lanthier M, Gregory KB, Lovley DR.** 2008. Growth with high planktonic biomass in *Shewanella oneidensis* fuel cells. FEMS Microbiol. Lett. **278**: 29–35.
18. **Lin WC, Coppi MV, Lovley DR.** 2004. *Geobacter sulfurreducens* can grow with oxygen as a terminal electron acceptor. Appl. Environ. Microbiol. **70**:2525–2528.
19. **Logan BE, Regan JM.** 2006. Electricity-producing bacterial communities in microbial fuel cells. Trends Microbiol. **14**:512–518.
20. **Lovley DR.** 2008. The microbe electric: conversion of organic matter to electricity. Curr. Opin. Biotechnol. **19**:564–571.
21. **Lovley DR, Phillips EJ.** 1987. Rapid assay for microbially reducible ferric iron in aquatic sediments. Appl. Environ. Microbiol. **53**:1536–1540.
22. **Marsili E, Sun J, Bond DR.** 2010. Voltammetry and growth physiology of *Geobacter sulfurreducens* biofilms as a function of growth stage and imposed electrode potential. Electroanalysis **22**:865–874.
23. **McKinlay JB, Zeikus JG, Vieille C.** 2005. Insights into *Actinobacillus succinogenes* fermentative metabolism in a chemically defined growth medium. Appl. Environ. Microbiol. **71**:6651–6656.
24. **Methé BA, et al.** 2003. Genome of *Geobacter sulfurreducens*: metal reduction in subsurface environments. Science **302**:1967–1969.
25. **Nevin KP, et al.** 2009. Anode biofilm transcriptomics reveals outer surface components essential for high density current production in *Geobacter sulfurreducens* fuel cells. PLoS One **4**:e5628.
26. **Pant D, Van Bogaert G, Diels L, Vanbroekhoven K.** 2010. A review of the substrates used in microbial fuel cells (MFCs) for sustainable energy production. Bioresour. Technol. **101**:1533–1543.
27. **Picioreanu C, van Loosdrecht MC, Heijnen JJ.** 1998. A new combined differential-discrete cellular automaton approach for biofilm modeling: application for growth in gel beads. Biotechnol. Bioeng. **57**:718–731.
28. **Picioreanu C, van Loosdrecht MC, Heijnen JJ.** 1998. Mathematical modeling of biofilm structure with a hybrid differential-discrete cellular automaton approach. Biotechnol. Bioeng. **58**:101–116.
29. **Pinchuk GE, et al.** 2009. Genomic reconstruction of *Shewanella oneidensis* MR-1 metabolism reveals a previously uncharacterized machinery for lactate utilization. Proc. Natl. Acad. Sci. U. S. A. **106**:2874–2879.
30. **Rabaey K, Boon N, Siciliano SD, Verhaege M, Verstraete W.** 2004. Biofuel cells select for microbial consortia that self-mediate electron transfer. Appl. Environ. Microbiol. **70**:5373–5382.
31. **Reguera G, et al.** 2005. Extracellular electron transfer via microbial nanowires. Nature **435**:1098–1101.
32. **Reguera G, et al.** 2006. Biofilm and nanowire production lead to increased current in microbial fuel cells. Appl. Environ. Microbiol. **72**: 7345–7348.
33. **Reguera G, Pollina RB, Nicoll JS, Lovley DR.** 2007. Possible nonconductive role of *Geobacter sulfurreducens* pilus nanowires in biofilm formation. J. Bacteriol. **189**:2125–2127.
34. **Ren Z, Ward TE, Regan JM.** 2007. Electricity production from cellulose in a microbial fuel cell using a defined binary culture. Environ. Sci. Technol. **41**:4781–4786.
35. **Richter H, et al.** 2009. Cyclic voltammetry of biofilms of wild type and mutant *Geobacter sulfurreducens* on fuel cell anodes indicates possible roles of OmcB, OmcZ, type IV pili, and protons in extracellular electron transfer. Energy Environ. Sci. **2**:506–516.
36. **Rollefson JB, Stephen CS, Tien M, Bond DR.** 2011. Identification of an extracellular polysaccharide network essential for cytochrome anchoring and biofilm formation in *Geobacter sulfurreducens.* J. Bacteriol. **193**: 1023–1033.
37. **Segura D, Mahadevan R, Juarez K, Lovley DR.** 2008. Computational and experimental analysis of redundancy in the central metabolism of *Geobacter sulfurreducens.* PLoS Comput. Biol. **4**:e36.
38. **Srikanth S, Marsili E, Flickinger MC, Bond DR.** 2008. Electrochemical characterization of *Geobacter sulfurreducens* cells immobilized on graphite paper electrodes. Biotechnol. Bioeng. Symp. **99**:1065–1073.
39. **Torres CI, et al.** 2010. A kinetic perspective on extracellular electron transfer by anode-respiring bacteria. FEMS Microbiol. Rev. **34**:3–17.
40. **Wolin MJ.** 1982. Hydrogen transfer in microbial communities. *In* Bull AT, Slater JH (ed), Microbial interactions and communities, vol 1. Academic Press, London, United Kingdom.
41. **Yang TH, Coppi MV, Lovley DR, Sun J.** 2010. Metabolic response of *Geobacter sulfurreducens* towards electron donor/acceptor variation. Microb. Cell Fact. **9**:90.